Hybrid-functional material for sorption-enhanced hydrogen-rich syngas production from biomass: Effect of material preparation process

Shujuan Zou[1,#], Weiguo Dong[2,#], Binhai Cheng[1,3,*], Yeshui Zhang[4], Paul T. Williams[5,*], Ming Zhao[1,3]

[1] School of Environment, Tsinghua University, Beijing 100084, China

[2] School of Management, China University of Mining and Technology (Beijing), Beijing 100083, China

[3] Research Institute for Environmental Innovation (Suzhou), Tsinghua, Suzhou215263, China

[4] Department of Chemical Engineering, University College London, London, UK, WC1E 7JE

[5]School of Chemical and Process Engineering, University of Leeds, Leeds, UK, LS2 9JT

(* Corresponding authors: p.t.williams@leeds.ac.uk; and bhcheng1@mail.ustc.edu.cn)

([#] Authors with equal contribution)

Abstract: Pyrolysis of waste biomass sawdust coupled with sorption-enhanced catalytic steam reforming of the pyrolysis gases has been investigated using a novel Ni-CaO-Ca_2SiO_4 hybrid-functional material for enhanced hydrogen production. Using hybrid stabilized materials with integrated sorption and catalysis functions overcomes the thermodynamic constraint of the reforming reaction equilibrium. The Ni-CaO-Ca_2SiO_4 hybrid-functional material was prepared under different catalyst drying methods to determine the influence on hydrogen yield. In addition, the process parameters of water injection rates, and catalytic temperature were investiugated to optimise the process. The results showed that the presence of Ni-CaO-Ca_2SiO_4 significantly improved the yield and volume fraction of syngas. The spray-dried hybrid-functional material was shown to be the most effective in terms of H_2 yield and purity in the syngas owing to its relatively high stability and higher surface area. The Ni-CaO-Ca_2SiO_4 material prepared using spray drying gave the highest H_2 yield of 25.75 mmol $g_{biomass}^{-1}$ that was eight times higher than the material-free test at a reforming temperature of 850 °C and water injection rate of 5 mL h^{-1}. Furthermore, the highest yield syngas (H_2 and CO) was also achieved under these conditions, and where the optimal calorific value of the total gaseous products was 10.63 kJ m^{-3}.

Keywords: biomass waste, steam gasification, hydrogen, two-stage fixed-bed reactor, hybrid-functional materials

1. Introduction

Developing new renewable energy has attracted major recent interest [1]. Biomass energy is an alternative to fossil fuels has a number of advantages as a renewable energy resource. For an example, biomass is rich in organic material with high volatile content which makes it suitable for thermochemical resource utilization to produce high-quality energy and contains lower amounts of nitrogen and sulfur minimising pollution of the environment [2,3]. It is also produced as waste biomass as the by-product of agriculture, forestry, and food-processing streams [4]. In particular, the waste can be converted into a gas product through gasification in the presence of gasifying agents [5]. Water steam is one of the most widely used gasifiers [6]. Additional addition of steam or retention of a proper amount of water in the feedstock can enhance catalytic activity and provide hydrogen production [7-8]. Syngas can be used as fuel to generate electricity or as raw material to synthesize chemicals such as ammonia and methanol [9,10]. Hydrogen is also regarded as a pollutant-free fuel and high calorific value energy source, and can be used in fuel cells, chemical synthesis, float glass etc. [11,12]. The development and application of hydrogen also provides a promising solution for mitigation of global warming as a low carbon fuel. The yield and quality of syngas or hydrogen generated from biomass determines the conversion efficiency of biomass energy.

Two-stage thermochemical processing of biomass, by pyrolysis of the biomass to produce a range of gases in the first stage followed by catalytic steam reforming/gasification of the pyrolysis gases in the second stage has proven to produce syngas or hydrogen [13]. Compared with the one-stage batch reactor system in which pyrolysis samples and catalysts are mixed, the two-stage fixed bed reactor system is favorable for catalyst recovery. In addition, pyrolysis requires a lower temperature than catalytic steam reforming/gasification, so the two stage system allows for separate temperature controlled reactors. Also, the two-stage reactor ensures better interaction between pyrolysis gases and the catalyst. For the two-stage fixed-bed reactor, the catalyst is one of the most important parameters to affect gas production

Sorption-enhanced catalytic steam reforming of biomass consists of catalytic reforming and CO_2 adsorption for syngas and hydrogen production [14-17]. In our previous work, a hybrid-functional material in the form of Ni-CaO-Ca_2SiO_4 was developed for sorption-enhanced catalytic steam reforming of biomass and showed enhanced hydrogen production performance and cyclic stability [18]. It has been reported that during the preparation of multifunctional sorption/catalytic materials, the drying method of the materials has been shown to strongly influence their structure and activity [19-21]. For examples, Moom et al. found that the performance of a freeze dried catalyst (NiCo-CeZr) was better than an oven dried catalyst for the conversion of methane to H_2/CO in the dry

reforming of CH_4 with CO_2 [19]. Le et al. reported that catalyst synthesis by spray drying was not only a fast process but also showed high reproducibility [20]. Driessche et al. confirmed that the spray drying method was conducive to the formation of uniform particles of $Bi_{2-x}Pb_xSr_2Ca_2Cu_3O_y$ [21].

In this work, a hybrid-functional material, Ni-CaO-Ca_2SiO_4, was used in a two-stage fixed-bed reactor for the pyrolysis-catalytic steam reforming of biomass waste. To explore the effect of drying methods on material structure and catalytic activity, the materials prepared by spray drying, oven drying spray and freeze drying were investigated. The influence of process parameters, water injection rate and reforming temperature were also investigated for the optimization of the process. This work provides an important basis for the large-scale application of steam gasification technology with the hybrid-functional material, Ni-CaO-Ca_2SiO_4.

2. Materials and methods

2.1 Feedstock and catalysts

The biomass used was obtained from Liverpool Wood Pellets Ltd., Liverpool, UK in the form of waste wood pellets which were shredded and sieved to produce sawdust

(average particle size ~0.2 mm). Table 1 shows the results of proximate and ultimate analysis of the sawdust. The liquid precursor for manufacture of the Ni-CaO-Ca_2SiO_4 hybrid-functional material was synthesized from tetraethyl orthosilicate, nitric acid, calcium acetate, and nitrate hexahydrate. Firstly, 5 mmol pure tetraethyl orthosilicate was added to 1mmol L^{-1} nitric acid and stirred in a magnetic stirrer at 600 min^{-1} for 40 minutes until the mixed solution was completely dissolved. 45 mmol calcium oxalate and nitrate hexahydrate were added to the mixed solution in sequence to obtain the liquid precursor. Specific synthesis methods were described in detail in our previous work [18]. Then, the liquid precursor was dried by three methods: freeze drying, oven drying, and spray drying.

Oven drying is a conventional method of direct heating of the liquid precursor with simultaneous stirring with a magnetic heating agitator at 80 °C until a slurry is developed for oven drying [22-24]. During the spray drying process, the solution precursor was atomized to small particles into the drying chamber, where the moisture rapidly evaporated when contacting the hot air ~300 °C. In the freeze drying process, the liquid precursor was frozen and sealed at -80 °C under vacuum. The liquid precursor is dried by sublimation of ice to water vapor [12].

The material samples dried by the different methods were calcined at 750 °C thermostatically for 2 h after the drying process with a heating rate of 20 °C min^{-1} in air followed by sieving to produce particles in a range between 50 μm to 212 μm. In order to

achieve high catalytic efficiency, all catalysts were reduced under a mixture of 5 vol % H_2 and 95 vol.% N_2 for 2 h at 800 °C.

2.2 Material characterization

The crystal structures of the fresh hybrid-functional materials were identified by X-ray diffraction (XRD) using a Rigaku Dmax/2500 XRD with a scanning angle of 10-90° (8° min^{-1}) and a Cu, Ka X-ray radiation at wavelength 0.1542 nm. The morphology of the produced materials was obtained by scanning electron microscopy (SEM) using a JSM-5610LV, JEOL, instrument coupled with elemental content analysis using an energy dispersive X-ray spectrometer (EDXS). The specific surface area, total pore volume and pore size distribution of the materials prepared using the three drying methods were obtained by N_2 adsorption–desorption isotherms using a Quanta chrome auto sorb-i Q-C instrument. The specific surface area was calculated by the Brunauer, Emmett and Teller (BET) method, and BJH was used to calculate the total pore volume and pore size distribution.

2.3 Pyrolysis-catalytic steam reforming reactor system

The two-stage fixed-bed pyrolysis-catalytic steam reforming reactor system used for producing syngas and hydrogen from biomass is shown as a schematic diagram in Figure 1. The reactors were constructed of stainless steel each was 160 mm in length with an internal diameter of 22 mm, with each stage independently electrically heated and temperature controlled. In order to minimize the mutual influence of temperature on the two stages, the biomass sample crucible was hung at the center of the pyrolysis reactor. The condensation system is composed of air-cooling to perform initial condensation at ambient temperature followed by a dry ice condenser maintained at -78 °C which ensures condensation of the condensable hydrocarbons. N_2 was used as purge carrier gas with a flow rate of 100 mL min^{-1}. Before starting experiments, the catalytic reactor stage was first preheated to the set temperature before the start of pyrolysis. The waste biomass sawdust was placed in the sample crucible in the pyrolysis reactor and heated at a heating rate of 40 °C min^{-1} to the final temperature of 600 °C. Water was added to the second stage catalytic reactor by a syringe pump that immediately evaporated the water into steam at high temperature. The volatiles produced by pyrolysis of the biomass pass through the catalytic reactor where the Ni-CaO-Ca_2SiO_4 was placed, where reforming/gasification reactions occur. The product gases passing through the condensation system were collected

by a gas sample bag and analyzed off-line by gas chromatography (GC).

2.4 Analytical methods

The permanent gases (H_2, CO, O_2, and N_2) and CO_2 collected in the gas sample bag were analyzed by a Varian 3380 gas chromatograph with the same thermal conductivity detector but different molecular sieve columns, a 60-80 mm mesh packing for permanent gases, and 80-100 mm mesh packing for CO_2. Hydrocarbons including C_1-C_4 were detected by a separate Varian CP-3380 GC with flame ionization detection and 80-100 mm mesh HayeSep column. The total mass of gaseous products was calculated by the data from the GC. The mass of char was obtained by the mass difference of the pyrolysis stage sample crucible before and after the experiments. The mass difference of the condenser before and after gasification was recorded as the product liquid. The quantity of tar/bio-oil was calculated by difference based on the char and gas data in relation to the mass of biomass feedstock.

The lower heating value (LHV) of the product gas represented the heat released by the fuel gas during combustion and was calculated by [25]:

$$\mathrm{LHV} = (25.7\mathrm{X}_{\mathrm{H}_2} + 30\mathrm{X}_{\mathrm{CO}} + 85.4\mathrm{X}_{\mathrm{CH}_4} + 151.3 \times \mathrm{X}_{C_nH_m}) \times 4.2 \qquad \text{（Eq.1）}$$

$\mathrm{X}_{\mathrm{H}_2}\mathrm{X}_{\mathrm{CO}}\mathrm{X}_{\mathrm{CH}_4}\mathrm{X}_{C_nH_m}$: molar fraction of H_2, CO, CH_4 and C_nH_m.

3. Results and discussion

3.1 Materials characterization

The crystal structure of the hybrid-functional materials prepared by the three different drying methods were determined using XRD and the diffraction spectra results are shown in Figure 2. All of the diffraction peaks of Ni, CaO, and Ca2SiO4 are clearly observed, which demonstrates the presence of these three crystallographic particles in all three materials. The sizes of the crystallographic particles were calculated according to the Scherrer equation and the results are shown in Table 2. As can be seen from the data, the crystal spacing of CaO and Ca2SiO4 crystallographic particles by freeze drying and spray drying were much smaller than those of oven drying. This is due to the influence of liquid surface tension, molecular agglomeration occurs when solutes precipitating by oven drying. Spray drying and freeze drying have less significant liquid surface tension and molecular agglomeration. Water would be evaporated in-situ during the freeze drying process, and the precursor solution was dispersed into tiny droplets before evaporation during the spray drying process. So, oven drying had the largest crystal spacing [26].

The SEM and EDXS elemental mapping images of the hybrid-functional materials by the oven, spray and freeze drying methods are shown in Figure 3, showing the distribution

of the Ni, Ca and Si elements from EDXS mapping images. The three elements were visible and mixed, which confirmed the presence of Ni, Ca, and Si as a mixing. However, different drying methods correspond to different mixing uniformity. The oven-dried material showes obvious color block aggregation, which represents relatively poor dispersion. The spray drying and freeze drying processes may lead to a more porous structure as indicated by the surface area data shown in Table 3. The oven-dried particles also appeared to be agglomerated from the SEM image (Figure 3b). This could be explained as the liquid surface tension occurred at the gas-liquid interface, resulting in a downward force to the nearby particles followed by the coalescence of all particles [27]. However, freeze drying and spray drying avoid the pore structure collapse caused by surface tension. As mentioned above, water would be evaporated in-situ during the freeze drying process, so the gaps between the particles were well preserved. The precursor solution was dispersed into tiny droplets before evaporation during the spray drying process, therefore the pore structure was well preserved [28,29].

The adsorption-desorption isotherms of oven-dried material in Figure 4b showed a kind of concave adsorption curve (Type Ⅴ), in which the adsorption gas volume increases with the increase of component pressure. It was the typical physical adsorption process of mesoporous or macroporous adsorbents combined with Figure 4d. Figure 4a 4b and 4c show that the materials by three drying methods had adsorption hysteresis loops which was

a typical feature of mesoporous capillary aggregation [30]. The details of the void system of samples prepared by three drying methods were shown in and Table 3. It indicated that the specific surface area of the spray dried material was slightly higher than that of freeze dried material and nearly 5 times higher than that of the oven-dried material. So, the freeze drying and spray drying methods used for Ni-CaO-Ca2SiO4 material preparation were more beneficial than oven drying. More importantly, the pore size distribution in Figure 4d showed that there were abundant pores between 30 to 40 nm existing in all the three materials, but, the freeze dried and spray dried materials possessed many pores below 5 nm, while the oven-dried material did not show the presence of these smaller pores. The classification of porosity defines micropores (pore size <2 nm), mesopores (2-50 nm), and mesopores (>50 nm). The results suggested that freeze drying and spray drying methods could increase the specific surface area by generating more pores below 5 nm.

3.2 Effect of sorption-catalyst drying methods on catalyst activity

The materials prepared by the three different drying methods were applied as sorption enhanced catalyst hybrid functional materials for the biomass sawdust pyrolysis-catalytic reforming process with the two-stage fixed-bed reactor. For the experiments, the final pyrolysis stage temperature, 600 °C, the catalyst/sorption stage temperature was 850 °C and the water injection rate was 5 mL h^{-1}. The results are shown in Figure 5. The spray

dried material produced the highest hydrogen purity and hydrogen yield at 53.93 vol.% and 25.75 mmol $g_{biomass}^{-1}$, respectively. The oven-dried material showed a similar hydrogen purity and yield (53.8 vol.%, 24.93 mmol $g_{biomass}^{-1}$), whereas the freeze dried material showed the lowest purity and yield (50.84 vol.%, 19.03 mmol $g_{biomass}^{-1}$). The results suggest that the different drying methods affected the sorption-catalytic effective performance of the material by the development of different pore structures [31].

During the experiments, pyrolysis volatiles produced from the pyrolysis of biomass reacted with steam in the presence of the active Ni and CaO of the hybrid functional material that was attached to the surface of the Ca_2SiO_4. The larger the pore surface area of the catalyst-sorption material suggests that there will be more reaction sites available for reaction, which represents improved catalytic and CO_2 capture performance [32,33]. The spray-dried material had a larger surface area than the oven-dried material, which suggests the reason for higher catalytic performance in relation to hydrogen purity and yield [34]. However, the freeze-dried material had a similar surface area (35.5 m^2 g^{-1}) to the spray dried material and significantly higher than the oven-dried material, but exhibited the lowest hydrogen purity and yield (Figure 5). The reason may be that the freeze-dried material had poor stability under the thermal conditions of the experiments, and some structural changes may have occurred during the mass transfer and reaction processes. Manovic and Anthony proposed a "skeletal theory" which could further provide a

theoretical explanation for the experiment results [35]. They suggested that CaO had a "hard skeleton" supporting the material structure and a "soft skeleton" that reacted rapidly with gases during the process of CO_2 capture. The hard skeleton supported and maintained the basic structure of material particles and the reactive soft skeleton was the main area of bulk diffusion. In this work, this theory has been summarized as a stereogram, as shown in Figure 6. Song et al. further applied this theoretical model to explain the structure of different drying methods of CaO [27]. Freeze drying had a pre-freezing process of the liquid precursor for a sufficient period of time to form dendritic ice crystals, and the moisture was evaporated directly into vapor in-situ under vacuum in a dry state, and a fine porous structure was easily formed. Oven drying formed compacted materials due to the effect of surface tension, and spray drying, after dispersing the liquid as tiny droplets, was dried quickly, so the porous structure which had uniform shape was easily formed. Song et al. suggested that the structure formed by freeze drying lacked the support of the hard skeleton, and was mostly formed by a soft skeleton, so it was not stable enough during reaction [27]. This theory also applies well in this work, although the fresh freeze-dried material had a larger surface area than that of the oven-dried material, its poor stability determined that its catalytic-adsorption performance in the experiments was poor. Spray drying particles were relatively uniform, with fine pore structure and good soft skeletons, at the same time, the particles had sufficient hard skeletons to support the material structure,

so the spray dried material showed the best catalytic-adsorption properties in relation to hydrogen gas purity and hydrogen yield.

With the same temperature and water injection rate (850 °C, 5ml h^{-1}), the total gas production was maintained within 74~78 wt.% for the different drying methods. The results have demonstrated that the method of drying of the materials was not the main factor affecting the total gas production, but had a significant impact on the product gas composition, mainly in terms of hydrogen yield and purity. The spray-dried material was the most effective in terms of the promotion of hydrogen gas purity and hydrogen yield, and was selected for subsequent experiments to optimize the process conditions.

3.3 Effect of water injection rate on gas production.

The effect of water injection rate into the second stage catalytic reactor was investigated using the spray dried preparation process for the Ni-CaO-Ca_2SiO_4 in the pyrolysis-catalytic reforming/sorption process using the two-stage fixed-bed reactor. The pyrolysis stage final temperature was 600 °C and the second stage catalyst/sorption reactor temperature was 850 °C.

The results in relation to product yield, gas yield and gas composition for the pyrolysis-catalytic steam reforming/sorption of the waste biomass with different water injection rates from 0 to 5 mL h^{-1} are shown in Figure 7. The purity and yield of hydrogen

gas improved with the increase of water injection rate and reached a peak at the water injection rate of 5 mL h^{-1}, producing a hydrogen volumetric gas composition of 53.93 vol.% and a hydrogen yield of 25.75 mmol $g_{biomass}^{-1}$. In addition, as the water injection rate was increased, the CO_2 yield also increased, and CO yield declined, since the CO reacted with steam to produce CO_2 and H_2 (water gas shift reaction) (Eq. 2), in which the steam was used as a gasifying agent to supply elemental hydrogen.

$$CO + H_2O \rightarrow CO_2 + H_2 \qquad \text{(Eq.2)}$$

CO_2 generated by the pyrolysis of biomass and produced during the catalytic steam reforming and water gas shift reactions has also been reported as a reforming agent for biomass as 'dry reforming' [36].

$$C_nH_m + nCO_2 \rightarrow 2nCO + \frac{m}{2}H_2 \qquad \text{(Eq. 3)}$$

But with the increase of CO and H_2 and the decrease of CO_2, suggests that dry reforming may also be occurring. It is also worth noting that there were other chemical reactions that might occur (Eq. 4 and Eq. 5) [37].

$$C + CO_2 \rightarrow 2CO \qquad \text{(Eq. 4)}$$

$$CO + CO_2 + 7H_2 \rightarrow 2CH_4 + 3H_2O \qquad \text{(Eq. 5)}$$

Comparing the lower heating values (LHVs) of the gaseous product, it was shown that when the water injection rate was 0 mL h^{-1}, the LHV was the highest, at 11.05 MJ/Nm^{-3}. As the water injection rate was increased, the LHV of the product gas decreased. Because

the main chemical reaction in this experiment was the water gas shift (WGS) reaction, which was an exothermic reaction. Therefore, the LHV of the product gases dropped when the water injection rate was increased from 0 mL h^{-1} to 2 mL h^{-1}, but when the water injection was further increased from 2 mL to 5 mL the rate of decline in the LHV was reduced.

3.4 Effect of temperature on gas production.

The effect of temperature of the second stage reactor containing the Ni-CaO-Ca_2SiO_4 catalyst/sorption hybrid material prepared using the spray dried preparation process was investigated using the two-stage fixed-bed reactor. Temperature is a critical influencing factor for all three major types of reactions, reforming reaction, carbonation, and water gas shift reactions in the steam gasification process. The effect of catalyst/sorption temperature on gas production was systematically investigated by varying the catalyst/sorption stage temperature from 550 °C to 850 °C. Table 4 shows the related results of product yield, gas yield and composition. As the temperature was increased, the total gas production also increased. Increased temperature also facilitated the removal of tar/bio-oil. As the catalyst/sorption temperature was increased from 550°C to 850°C, the total gas production was increased from 0.32 wt.% to 0.78 wt.%. The H_2 and CO yield reached a peak at 850 °C

at 25.75 mmol $g_{biomass}^{-1}$ and 13.25 mmol $g_{biomass}^{-1}$ respectively. At the same time, the yields of C_nH_m and CH_4 were declining, and the yield of CO and H_2 rose because the elevated temperature promoted the catalytic activity of Ni facilitating reforming reactions, resulting in more CO and H_2 produced. This conclusion was consistent with the study by Courson et al. who reported that increasing the catalyst temperature from 400 °C to ~800°C， the activity of the Ni-based catalyst was improved for hydrogen production from biomass [38].

In these experiments, the effects of temperature on the various reactions that occur between the multi-functional material components and the biomass pyrolysis gases will be different because of the differences in thermodynamic equilibrium of the different reactions. Baker et al. studied the adsorption of carbon dioxide by calcium oxide at different pressures of 1 to 300 atm [39]. The ability of CaO to adsorb CO_2 was related to the partial pressure of CO_2 and reaction temperature [39]. Song et al. found that CaO exhibited the highest CO_2 capture ability at a reaction temperature of 700 °C in a 15% CO_2 atmosphere [40]. From Table 4, the results show that as the catalyst/sorption temperature was increased, the CO_2 yield and volumetric concentration increased, and the H_2 vol.% concentration decreased. The produced $CaCO_3$ started to release CO_2 at a high temperature of more than 800 °C, resulting in an increase in the volumetric concentration of CO_2 and a decrease in H_2 [41]. Furthermore, at higher reaction temperatures of 750 °C and 850 °C, continuous accumulation of CO_2 possibly adversely affected the water gas shift reaction. Li et al.

investigated the effects of temperature on the water gas shift reaction with Ni-based catalyst and found that the percentage CO conversion reached ~1 at 400 °C [42].

Through evaluation of the data from Table 4, even if the purity of H_2 decreased with increasing temperature, the syngas yield and volume fraction, H_2 yield, total yield and heat of gas all reached their highest at 850 °C and with a water injection rate of 5mL h^{-1}. Compared with the catalyst-free experiment with the same temperature and water injection rate, the presence of Ni-CaO-Ca_2SiO_4 material improved the yield of H_2 by more than eight times, increasing from 3.16 mmol $g_{biomass}^{-1}$ to 25.75 mmol $g_{biomass}^{-1}$. In addition, the syngas yield increased from 8.6 mmol $g_{biomass}^{-1}$ to 39 mmol $g_{biomass}^{-1}$, and the volumetric gas concentration of the syngas increased from 60.77 vol.% to 81.69 vol.%. Also, the gas yield and total calorific value of gas have also been greatly improved.

4. Conclusions

In this work, the application of a hybrid-functional material, Ni-CaO-Ca_2SiO_4, in a two-stage fixed-bed biomass pyrolysis-catalytic/sorption reactor system markedly increased the production of hydrogen, compared to a non-catalytic reaction. The effects of three drying methods (oven drying, spray drying and freeze drying) employed in the manufacture of the hybrid material on the catalytic/sorption performance of the material have been studied. Spray drying was beneficial for the formation of mesopores and material

stability in the produced hybrid Ni-CaO-Ca_2SiO_4 material which was linked to the high yield of hydrogen and syngas from this material.

Further optimization of the pyrolysis-catalytic/sorption process for the production of hydrogen and syngas from biomass using the spray dried Ni-CaO-Ca_2SiO_4, was carried out, investigating the influence of water injection rate and catalytic/sorption temperature. The higher the water steam input, the higher the yield and volumetric gas concentration of H_2 that was produced. The increase of catalytic/sorption temperature promoted the total yield and the optimal calorific value of the gaseous products, the yield and volume fraction of syngas, and the H_2 yield. In this study, the optimal parameters of 5mL min^{-1} water injection rate and catalytic/sorption temperature of 850 °C were found to produce the optimal gaseous products (highest H_2 yield of 25.75 mmol$g_{biomass}^{-1}$, as well as highest syngas yield of 39 mmol $g_{biomass}^{-1}$ and volumetric gas concentration of 81.69 vol.%) using the spray-dried hybrid-functional material.

Acknowledgements

This work was supported by the National Key Research and Development Program of China（2019YFC1904602 and the Key Sci-Tech Innovation 2025 Program of Ningbo, China (2018B10025).

REFERENCES

[1]. Owusu P. A.; Asumadu-Sarkodie S.; Dubey S., A review of renewable energy sources, sustainability issues and climate change mitigation. *Cogent Engineering* **2016**, 3, (1), 1167990.

[2]. Field, C. B.; Campbell, J. E.; Lobell, D. B., Biomass energy: the scale of the potential resource. *Trends in Ecology & Evolution* **2008,** 23, (2), 65-72.

[3]. Liu, W.-J.; Li, W.-W.; Jiang, H.; Yu, H.-Q., Fates of Chemical Elements in Biomass during Its Pyrolysis. *Chemical Reviews* **2017,** 117.

[4]. Tuck, C. O.; Pérez, E.; Horváth, I. T.; Sheldon, R. A.; Poliakoff, M., Valorization of Biomass: Deriving More Value from Waste. *Science* **2012,** 337, (6095), 695-699.

[5]. Qadi, N.; Takeno, K.; Mosqueda, A.; Kobayashi, M.; Motoyama, Y.; Yoshikawa, K., Effect of Hydrothermal Carbonization Conditions on the Physicochemical Properties and Gasification Reactivity of Energy Grass. *Energy & Fuels* **2019,** 33.

[6]. Vagia, E. C.; Lemonidou, A. A., Thermodynamic analysis of hydrogen production via steam reforming of selected components of aqueous bio-oil fraction. *International Journal of Hydrogen Energy* **2007,** 32, (2), 212-223.

[7]. Neumann J.; Binder S.; Apfelbacher A.; Gasson J.R.; Ramírez García P.; Hornung A., Production and characterization of a new quality pyrolysis oil, char and syngas from digestate – Introducing the thermo-catalytic reforming process. *Journal of Analytical and Applied Pyrolysis* **2015**, 113, 137-142.

[8]. Elmously M.; Jäger N.; Apfelbacher A.; Daschner R.; Hornung A., Thermo-Catalytic Reforming of spent coffee grounds. *Bioresources and Bioprocessing* **2019**, 6, 44.

[9]. Fang, K.; Li, D.; Lin, M.; Xiang, M.; Wei, W.; Sun, Y., A short review of heterogeneous catalytic process for mixed alcohols synthesis via syngas. *Catalysis Today* **2009,** 147, (2), 133-138.

[10]. Martínez, J. D.; Mahkamov, K.; Andrade, R. V.; Silva Lora, E. E., Syngas production in downdraft biomass gasifiers and its application using internal combustion engines. *Renewable Energy* **2012,** 38, (1), 1-9.

[11]. Dutta, S., A review on production, storage of hydrogen and its utilization as an energy resource. *Journal of Industrial and Engineering Chemistry* **2014,** 20, (4), 1148-1156.

[12]. Sinigaglia, T.; Lewiski, F.; Santos Martins, M. E.; Mairesse Siluk, J. C., Production, storage, fuel stations of hydrogen and its utilization in automotive applications-a review. *International Journal of Hydrogen Energy* **2017,** 42, (39), 24597-24611.

[13]. Williams E.A., Williams P.T, The pyrolysis of individual plastics and a plastic mixture in a fixed bed reactor. *Journal of Chemical Technology & Biotechnology*

1997, 70, (1), 9-20.

[14]. Florin, N. H.; Harris, A. T., Hydrogen production from biomass coupled with carbon dioxide capture: The implications of thermodynamic equilibrium. *International Journal of Hydrogen Energy* **2007,** 32, (17), 4119-4134.

[15]. Huang, B.-S.; Chen, H.-Y.; Chuang, K.-H.; Yang, R.-X.; Wey, M.-Y., Hydrogen production by biomass gasification in a fluidized-bed reactor promoted by an Fe/CaO catalyst. *International Journal of Hydrogen Energy* **2012,** 37, (8), 6511-6518.

[16]. Cruz-Hernández, A.; Mendoza-Nieto, J. A.; Pfeiffer, H., NiOCaO materials as promising catalysts for hydrogen production through carbon dioxide capture and subsequent dry methane reforming. *Journal of Energy Chemistry* **2017,** 26, (5), 942-947.

[17]. Dang, C.; Li, Y.; Yusuf, S. M.; Cao, Y.; Wang, H.; Yu, H.; Peng, F.; Li, F., Calcium cobaltate: a phase-change catalyst for stable hydrogen production from bio-glycerol. *Energy & Environmental Science* **2018,** 11, (3), 660-668.

[18]. Ji, G.; Xu, X.; Yang, H.; Zhao, X.; He, X.; Zhao, M., Enhanced Hydrogen Production from Sawdust Decomposition Using Hybrid-Functional Ni-CaO-Ca_2SiO_4 Materials. *Environmental Science & Technology* **2017,** 51, (19), 11484-11492.

[19]. Aw, M. S.; Osojnik Črnivec, I. G.; Djinović, P.; Pintar, A., Strategies to enhance dry reforming of methane: Synthesis of ceria-zirconia/nickel–cobalt catalysts by freeze-drying and NO calcination. *International Journal of Hydrogen Energy* **2014,** 39, (24), 12636-12647.

[20]. Le, M. T.; Van Craenenbroeck, J.; Van Driessche, I.; Hoste, S., Bismuth molybdate catalysts synthesized using spray drying for the selective oxidation of propylene. *Applied Catalysis A: General* **2003,** 249, (2), 355-364.

[21]. Van Driessche, I.; Mouton, R.; Hoste, S., Rapid formation of the Bi_2-$xPb_xSr_2Ca_2Cu_3O_y$ high Tc-phase, using spray-dried nitrate precursor powders. *Materials Research Bulletin* **1996,** 31, (8), 979-992.

[22]. Zhang, Y.; Williams, P.T., Carbon nanotubes and hydrogen production from the pyrolysis catalysis or catalytic-steam reforming of waste tyres. *Journal of Analytical and Applied Pyrolysis* **2016,** 122, 490-501.

[23]. Zhang, Y.; Wu, C.; Nahil, M. A.; Williams, P.T., Pyrolysis–Catalytic Reforming/Gasification of Waste Tires for Production of Carbon Nanotubes and Hydrogen. *Energy & Fuels* **2015,** 29, (5), 3328-3334.

[24]. Zhang, Y.; Wu, C.; Nahil, M. A.; Williams, P.T., High-value resource recovery products from waste tyres. *Proceedings of the Institution of Civil Engineers - Waste and Resource Management* **2016,** 169, (3), 137-145.

[25]. Lv, P. M.; Xiong, Z. H.; Chang, J.; Wu, C. Z.; Chen, Y.; Zhu, J. X., An experimental study on biomass air–steam gasification in a fluidized bed. *Bioresource Technology* **2004,** 95, (1), 95-101.

[26]. Vehring R, Foss WR, Lechuga-Ballesteros D. Particle formation in spray drying. *Journal of Aerosol Science* 2007;38:728-46.

[27]. Song, Y.; Ji, G.; Zhao, X.; He, X.; Cui, X.; Zhao, M., Effects of Drying Methods on Wet Chemistry Synthesis of Al-Stabilized CaO Sorbents for Cyclic CO_2 Capture. *Energy & Fuels* **2017,** 31, (11), 12521-12529.

[28]. Abdelwahed, W.; Degobert, G.; Stainmesse, S.; Fessi, H., Freeze-drying of nanoparticles: Formulation, process and storage considerations. *Advanced Drug Delivery Reviews* **2006,** 58, (15), 1688-1713.

[29]. Maa, Y.-F.; Nguyen, P.-A.; Sweeney, T.; Shire, S. J.; Hsu, C. C., Protein Inhalation Powders: Spray Drying vs Spray Freeze Drying. *Pharmaceutical Research* **1999,** 16, (2), 249-254.

[30]. Yu J.; Lin M.; Tan Q.; Li J., High-value utilization of graphite electrodes in spent lithium-ion batteries: From 3D waste graphite to 2D graphene oxide. *Journal of Hazardous Materials* **2021**, 401, 123715.

[31]. Liu, L.; Wang, B.; Du, Y.; Borgna, A., Supported $H_4SiW_{12}O_{40}/Al_2O_3$ solid acid catalysts for dehydration of glycerol to acrolein: Evolution of catalyst structure and performance with calcination temperature. *Applied Catalysis A: General* **2015,** 489, 32-41.

[32]. Chen, J.; Wu, Q.; Zhang, J.; Zhang, J., Effect of preparation methods on structure and performance of $Ni/Ce_{0.75}Zr_{0.25}O_2$ catalysts for CH_4–CO_2 reforming. *Fuel* **2008,** 87, (13), 2901-2907.

[33]. Mattos, L. V.; Jacobs, G.; Davis, B. H.; Noronha, F. B., Production of Hydrogen from Ethanol: Review of Reaction Mechanism and Catalyst Deactivation. *Chemical Reviews* **2012,** 112, (7), 4094-4123.

[34]. Gryglewicz, G.; Stolarski, M.; Gryglewicz, S.; Klijanienko, A.; Piechocki, W.; Hoste, S.; Driessche, I. V.; Carleer, R.; Yperman, J., Hydrodechlorination of dichlorobiphenyls over $Ni–Mo/Al_2O_3$ catalysts prepared by spray-drying method. *Chemosphere* **2006,** 62, (1), 135-141.

[35]. Manovic, V.; Anthony, E. J., Thermal Activation of CaO-Based Sorbent and Self-Reactivation during CO_2 Capture Looping Cycles. *Environmental Science & Technology* **2008,** 42, (11), 4170-4174.

[36]. Hurley, S.; Li, H.; Xu, C., Effects of impregnated metal ions on air/CO_2-gasification of woody biomass. *Bioresource Technology* **2010,** 101, (23), 9301-9307.

[37]. Hecht, E. S.; Shaddix, C. R.; Geier, M.; Molina, A.; Haynes, B. S., Effect of CO_2 and steam gasification reactions on the oxy-combustion of pulverized coal char. *Combustion and Flame* **2012,** 159, (11), 3437-3447.

[38]. Courson, C.; Udron, L.; Świerczyński, D.; Petit, C.; Kiennemann, A., Hydrogen production from biomass gasification on nickel catalysts: Tests for dry reforming of methane. *Catalysis Today* **2002,** 76, (1), 75-86.

[39]. Baker, E. H., 87. The calcium oxide-carbon dioxide system in the pressure range 1-300 atmospheres. *Journal of the Chemical Society (Resumed)* **1962**, (0), 464-470.

[40]. Zhao, M.; Song, Y.; Ji, G.; Zhao, X., Demonstration of Polymorphic Spacing Strategy against Sintering: Synthesis of Stabilized Calcium Looping Absorbents for High-Temperature CO_2 Sorption. *Energy & Fuels* **2018,** 32, (4), 5443-5452.

[41]. Elias, K. F. M.; Lucrédio, A. F.; Assaf, E. M., Effect of CaO addition on acid properties of Ni–Ca/Al_2O_3 catalysts applied to ethanol steam reforming. *International Journal of Hydrogen Energy* **2013,** 38, (11), 4407-4417.

[42]. Li, Y.; Fu, Q.; Flytzani-Stephanopoulos, M., Low-temperature water-gas shift reaction over Cu- and Ni-loaded cerium oxide catalysts. *Applied Catalysis B: Environmental* **2000,** 27, (3), 179-191.

Table 1. Proximate and ultimate analysis of the waste biomass sawdust.

Proximate analysis(wt.% dry basis)	
Moisture	4.16
Volatile matter	76.24
Ash	1.48
Fixed carbon	18.12
Ultimate analysis(wt.% dry basis)	
C	48.12
H	7.24
O	44.20
N	0.44

Table 2. Lattice dimensions of Ni, CaO, $Ca(OH)_2$, and Ca_2SiO_4 from the oven dried, spray dried and freeze dried methods.

Drying methods	Ni (nm)	CaO (nm)	$Ca(OH)_2$ (nm)	Ca_2SiO_4 (nm)
Freeze drying	24.7	32.1	14.0	32.1
Oven drying	24.5	56.7	-	68.4
Spray drying	22.1	21.8	14.3	22.6

Ni:2θ=44.51°; CaO:2θ=32.12°,37.17°,53.86°; $Ca(OH)_2$: 2θ=34.02°; Ca_2SiO_4: 2θ=32.12°, 41.08°, 32.12°.

Table 3. BET specific surface area of the oven, spray and freeze dried sorption materials

Drying method	external surface area (m^2 g^{-1})	Pore volume (mL g^{-1})	Pore size (nm)
Freeze drying	33.513	0.406	3.191
Oven drying	7.021	0.099	3.171
Spray drying	35.502	0.412	3.192

Table 4. Product yield and gas yield and composition from the two-stage pyrolysis-sorption catalysis of biomass at different sorption-catalyst material temperatures.

		550°C	650°C	750°C	850°C	Catalyst-free
Volume fraction （%）	CO	15.08	18.82	22.2	27.76	38.24
	H_2	**61.59**	**58.51**	**54.76**	**53.93**	**22.53**
	CO_2	17.7	18.44	21.11	16.44	18.37
	CH_4	4.64	3.37	1.92	1.71	14.23
	C_nH_m	0.99	0.86	0.01	0.17	6.63
	CO+H_2	**76.67**	**77.33**	**76.96**	**81.69**	**60.77**
Yield (mmol $g_{biomass}^{-1}$）	CO	3.37	5.73	9.06	13.25	6.44
	H_2	**13.77**	**17.82**	**22.36**	**25.75**	**3.16**
	CO_2	3.96	5.62	8.62	7.85	2.98
	CH_4	1.04	1.03	0.78	0.81	2.39
	C_nH_m	0.16	0.24	0	0.08	0.89
	CO+H_2	**17.14**	**23.55**	**31.42**	**39**	**8.6**
Gas (g)		**0.32**	**0.47**	**0.69**	**0.78**	**0.4**
Tar (g)		0.48	0.31	0.1	0.02	0.41
Char(g)		0.2	0.22	0.21	0.2	0.19
MB(%)		101.58	98.48	97.69	96.7	95.27
LHV(MJ/Nm^3)		10.83	10.43	9.41	9.94	7.56
Total Calorific value (gas. kJm^3)		**5.41**	**7.11**	**8.6**	**10.63**	**3.19**

Material drying method: Spray drying; the pyrolysis stage temperature: 600 °C; water injection rate: 5 mL h^{-1}. Catalyst-free: no catalyst; pyrolysis stage temperature, 600 °C; catalyst stage temperature, 850 °C.

Total Heat (gas. kJ) $= \mathrm{LHV} \times n_{gas} \times 22.4 \times 10^{-3} n_{gas}$: The total molar mass of the gas.

FIGURE CAPTIONS

Figure 1. Schematic diagram of the two-stage fixed-bed pyrolysis-catalytic/sorption steam reforming reactor system

Figure 2. XRD spectra of spray-dried, oven-dried, and freeze-dried materials

Figure 3. SEM and EDXS elemental mapping images of the hybrid-functional materials, a) Freeze dried, b) oven dried, c) spray dried.

Figure 4. N_2 adsorption–desorption isotherms of the materials: a) freeze dried, b) oven dried, c) spray dried. d) pore-size distribution curves of the three materials.

Figure 5. Product yield, gas yield and composition for the pyrolysis-catalytic steam reforming/sorption of waste biomass with different drying methods materials. Pyrolysis stage temperature, 600 °C; catalyst stage temperature, 850 °C, water injection rate:5 mL h^{-1}. a) the volume fraction of gas composition; b) the mass balance of the experiments and LHV of total gas production; c) the yield of gas composition; d) the mass balance.

Figure 6. Soft and hard skeleton simulation diagram.

Figure 7. Product yield, gas yield and composition for the pyrolysis-catalytic steam reforming/sorption of waste biomass for the spray dried hybrid functional material. Pyrolysis stage temperature, 600 °C; catalyst stage temperature, 850 °C. **a**. the volume fraction of gas composition; **b**. the mass balance of the experiment and LHV of total gas production; **c**. the yield of gas composition; **d**. the product mass balance.

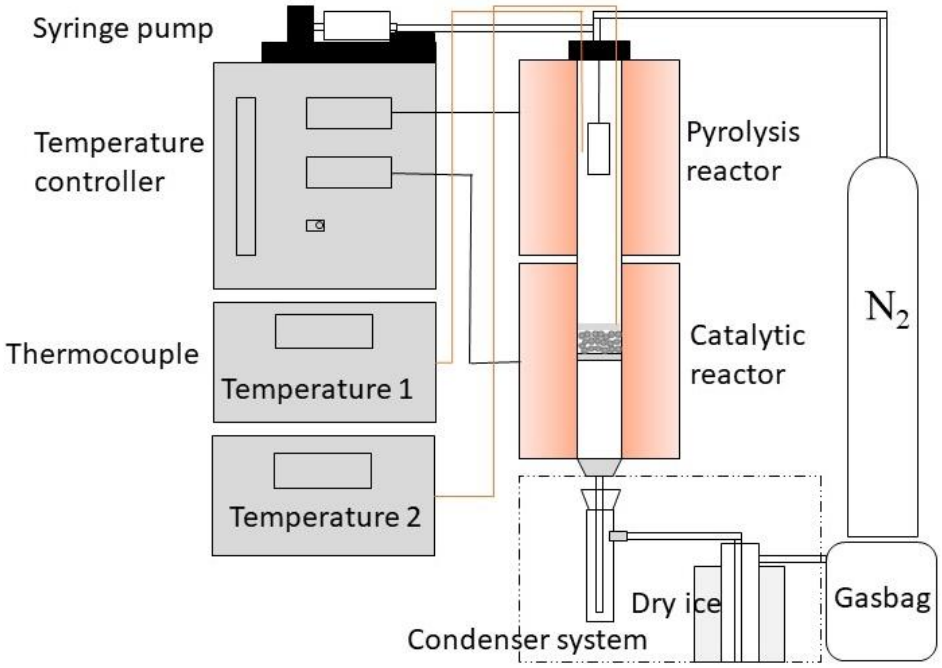

Figure 1. Schematic diagram of the two-stage fixed-bed pyrolysis-catalytic/sorption steam reforming reactor system

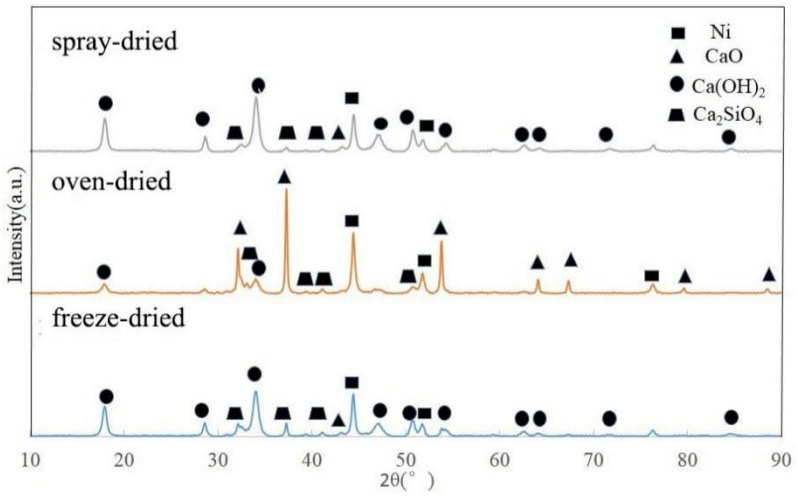

Figure 2. XRD spectra of spray-dried, oven-dried, and freeze-dried materials

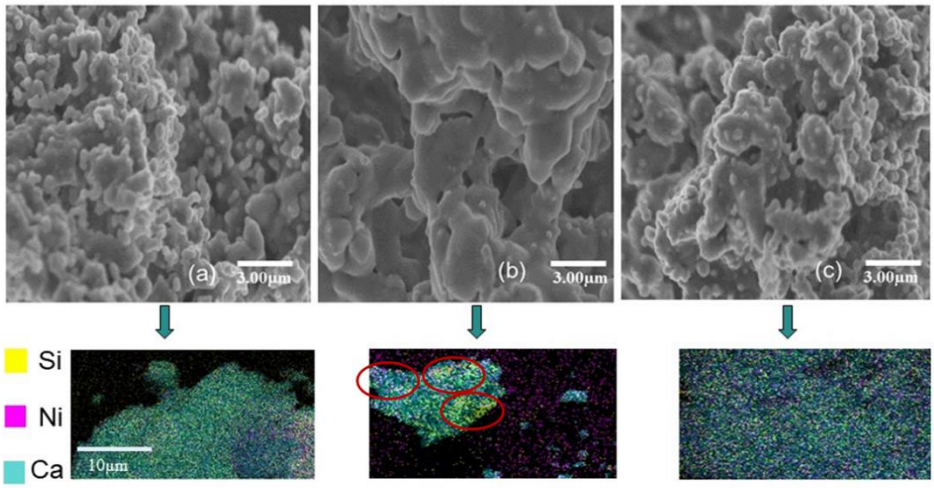

Figure 3. SEM and EDXS elemental mapping images of the hybrid-functional materials, a) Freeze dried, b) oven dried, c) spray dried.

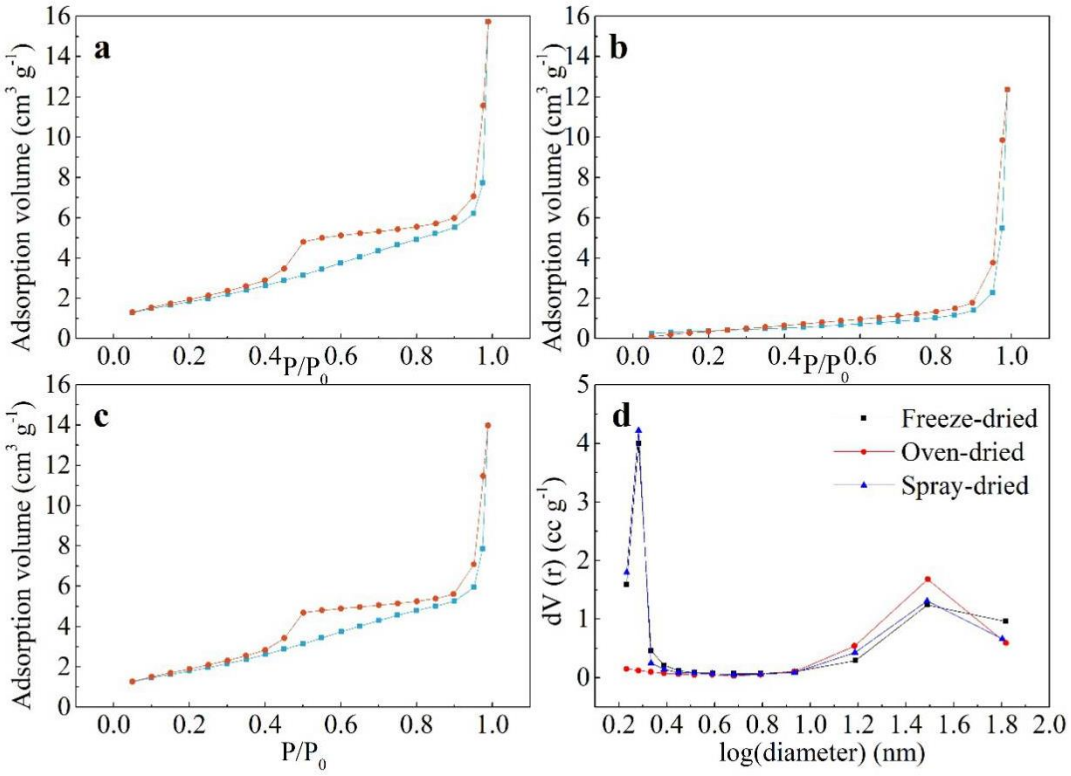

Figure 4. N_2 adsorption–desorption isotherms of the materials: a) freeze dried, b) oven dried, c) spray dried. d) pore-size distribution curves of the three materials.

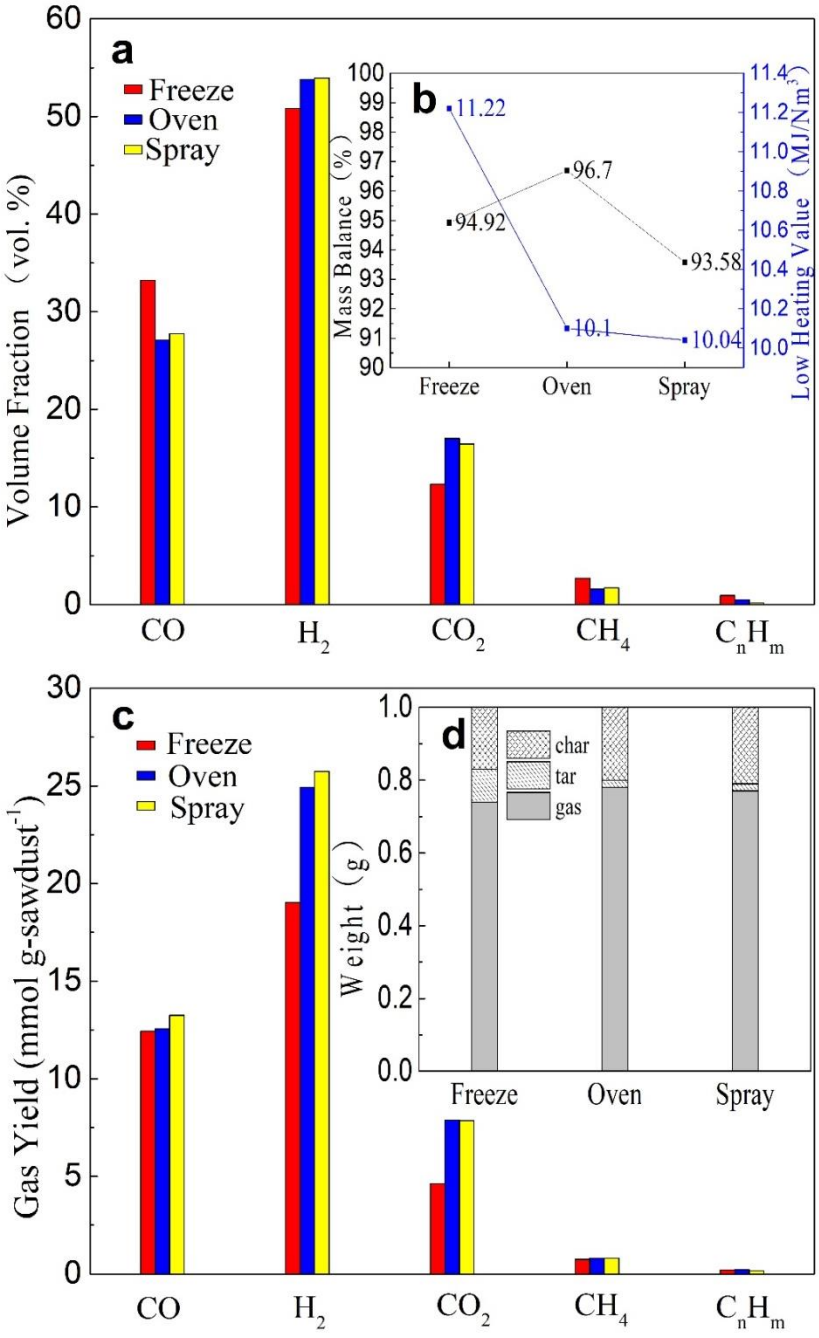

Figure 5. Product yield, gas yield and composition for the pyrolysis-catalytic steam reforming/sorption of waste biomass with different drying methods materials. Pyrolysis stage temperature, 600 °C; catalyst stage temperature, 850 °C, water injection rate:5 mL h^{-1}. a) the volume fraction of gas composition; b) the mass balance of the experiments and LHV of total gas production; c) the yield of gas composition; d) the mass balance.

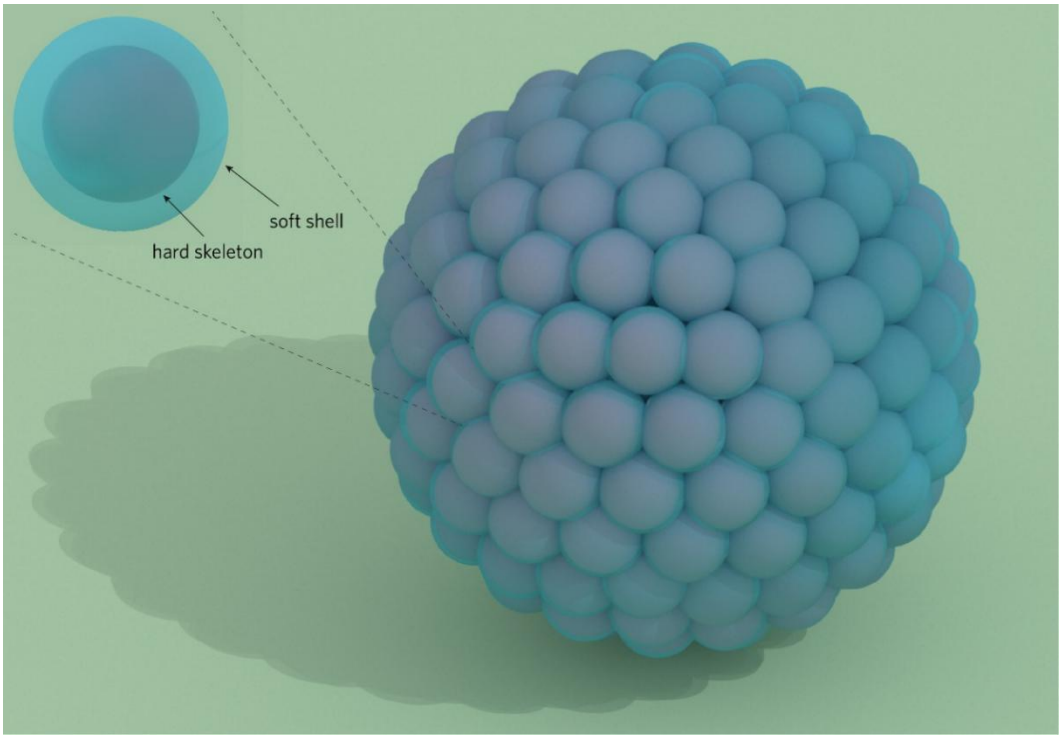

Figure 6. Soft and hard skeleton simulation diagram.

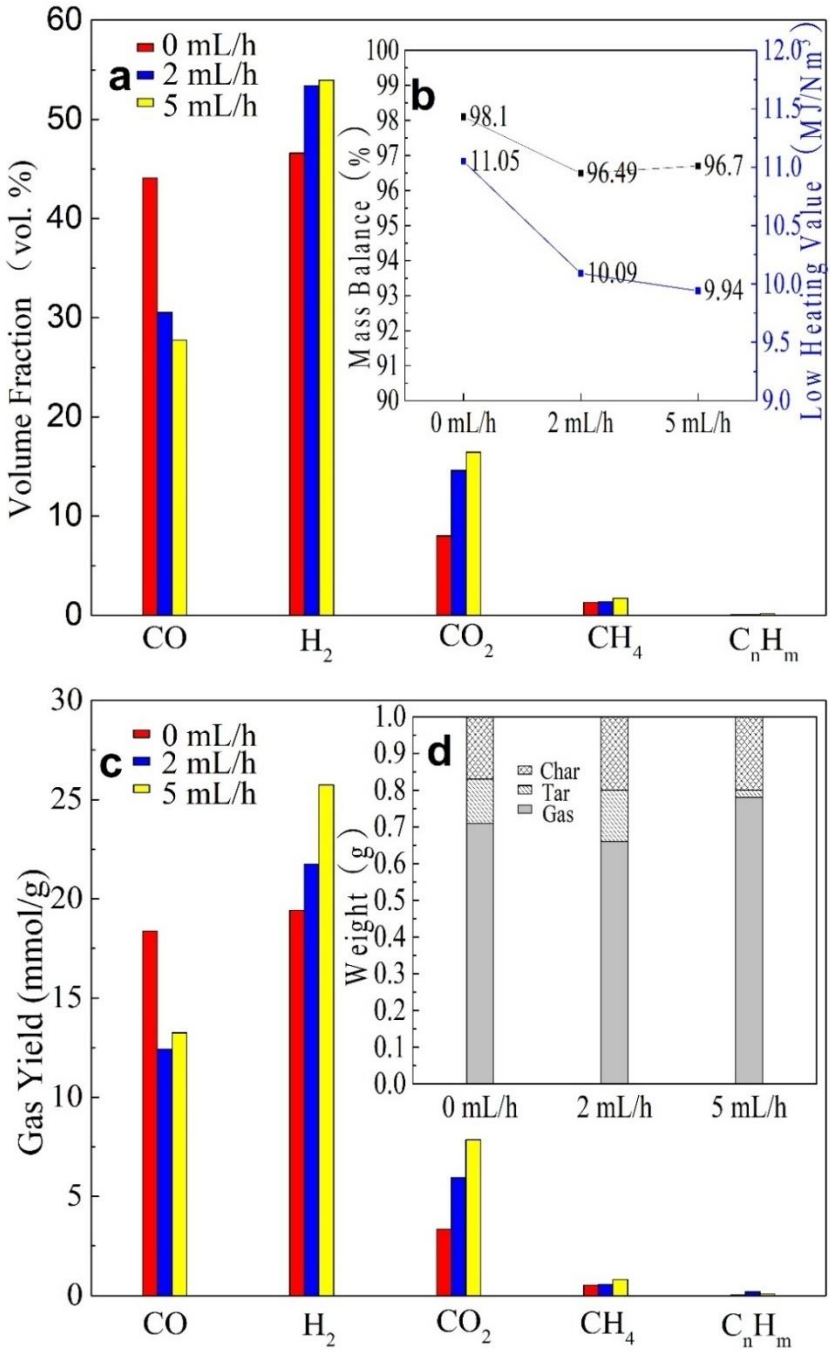

Figure 7. Product yield, gas yield and composition for the pyrolysis-catalytic steam reforming/sorption of waste biomass for the spray dried hybrid functional material. Pyrolysis stage temperature, 600 °C; catalyst stage temperature, 850 °C. **a**. the volume fraction of gas composition; **b**. the mass balance of the experiment and LHV of total gas production; **c**. the yield of gas composition; **d**. the product mass balance.